Fuel 90 (2011) 1999–2006

Contents lists available at ScienceDirect

Fuel

journal homepage: www.elsevier.com/locate/fuel

Combustion performance of bio-ethanol at various blend ratios in a gasoline direct injection engine

Dale Turner [a], Hongming Xu [a,*], Roger F. Cracknell [b], Vinod Natarajan [c], Xiangdong Chen [d]

[a] School of Mechanical Engineering, University of Birmingham, B15 2TT, UK
[b] Shell Global Solutions UK, Chester, UK
[c] Shell Global Solutions (US) Inc., Houston, TX, USA
[d] Jaguar Landrover, Coventry, UK

ARTICLE INFO

Article history:
Received 7 October 2010
Received in revised form 15 December 2010
Accepted 19 December 2010
Available online 5 January 2011

Keywords:
Ethanol
Gasoline
Combustion
SI engine

ABSTRACT

Bio-ethanol has the potential to be used as an alternative to petroleum gasoline for the purpose of reducing the total CO_2 emissions from internal combustion engines and this paper is devoted to the investigation of using different blending-ratios of bio-ethanol/gasoline with respect to spark timing and injection strategies. The experimental work has been carried out on a direct injection spark ignition engine at a part load and speed condition. It is shown that the benefits of adding ethanol into gasoline are reduced engine-out emissions and increased efficiency, and the impact changes with the blend ratio following a certain pattern. These benefits are attributed to the fact that the addition of ethanol modifies the evaporation properties of the fuel blend which increases the vapour pressure for low blends and reduces the heavy fractions for high blends. This is furthermore coupled with the presence of oxygen within the ethanol fuel molecule and the contribution of its faster flame speed, leading to enhanced combustion initiation and stability and improved engine efficiency.

1. Introduction

Bio-ethanol has been considered as an attractive fuel for internal combustion engines due to its renewable nature which provides both security of supply and reduced net CO_2 emissions. Other attractive properties include increased octane rating and enthalpy of vaporisation compared to standard gasoline, which allow for the use of increased compression ratios and the possibility of more favourable spark timings, increasing engine efficiency [1–3]. It is known that ethanol however has some significant drawbacks in terms of combustion and emission performances but the two most significant and problematic of these are the oxygenated nature of the fuel causing a reduction in lower heating value (~67% that of gasoline on a volume basis) and the reduced volatility of high ethanol blends coupled with the increased charge cooling can increase the cold start problems under severe weather conditions [4,5].

The study by Al-Farayedhi et al. [6] using a PFI injection strategy showed that the addition of ethanol to gasoline reduced the CO emissions, particularly for rich mixtures because of an increase in the available oxygen contained within the ethanol fuel molecule. It was also reported that the addition of 10%$_{Vol.}$ ethanol resulted in a reduction in NO_X emissions, but further increase in ethanol content caused an increase in NO_X emissions, though no data was given on combustion phasing. However the study by Wallner and Miers [3] showed that as the ethanol blend ratio was increased the NO_X emissions reduced with the cause being given as the increased enthalpy of vaporisation lowering the pre-combustion temperatures and the lower flame temperature of ethanol reducing the in-cylinder temperature as shown by a reduction in exhaust temperature. The addition of ethanol to gasoline has also been shown [3,6] to reduce hydrocarbon emissions, with the reduction increasing as the blend ratio is increased. The reason given for this is the reduction of the higher boiling point gasoline fractions in the fuel blend. Though this reduction could partially be attributed to the reduced sensitivity an FID has towards oxygenated hydrocarbons. Generally speaking, the effect of ethanol blends on NO_X emissions is not as conclusive as for unburned fuel emissions. It

Abbreviations: CAD, crank angle degrees; CID, combustion initiation duration; CLD, chemiluminescent detector; CO, carbon monoxide; CO_2, carbon dioxide; COV, coefficient of variation; DI, direct injection; EVC, exhaust valve closing; FID, flame ionisation detector; γ, ratio of specific heats; GE, gas exchange; HC, hydrocarbons; HRR, heat release rate; IMEP, indicated mean effective pressure; IVC, intake valve closing; IVO, intake valve opening; LHV, lower heating value; MBT, minimum advance for best torque; MFB, mass fraction burned; NDIR, non-dispersive infrared sensor; NO_X, oxides of nitrogen; PFI, port fuel injection; SoC, start of combustion; SoI, start of injection; ST, spark timing; TDC, top dead centre; VCT, variable cam timing.

* Corresponding author.
E-mail address: h.m.xu@bham.ac.uk (H. Xu).

0016-2361/$ - see front matter © 2010 Elsevier Ltd. All rights reserved.
doi:10.1016/j.fuel.2010.12.025

is believed that the increased charge cooling from ethanol can manifest itself in some engines with the result of lower in-cylinder temperatures and thus lower NO_X emissions.

It is widely reported [7–9] that ethanol has a higher laminar flame velocity than that of gasoline/iso-octane. The study by Hara and Tanoue [7] reports values of ~33 cm/s and ~39 cm/s respectively for gasoline and ethanol for stoichiometric mixtures at standard temperatures and pressures (100 kPa, 325 K). The study by Beeckmann et al. [8] at elevated temperatures and pressures (450 K, 304 kPa) gives values of ~24 cm/s and ~27 cm/s for iso-octane and ethanol respectively. The work by Farrell et al. [9] at a slightly elevated temperature of 373 K, but substantially increased pressure of 10 bar gives laminar flame velocities of ~58 cm/s and ~75 cm/s respectively for iso-octane and ethanol. Farrell et al. attributes this increase in velocity compared to non-oxygenated hydrocarbons (of similar carbon chain length) to the production of different intermediary species, particularly ethylene. Although these three different studies do not show clear temperature and pressure relationships they all do show that ethanol has a higher laminar flame speed than that of gasoline/iso-octane. Our own recent study [10] has compared the laminar burning velocities of ethanol, gasoline and the new bio-fuel candidate 2,5-dimethylfuran (DMF) at the same conditions for initial temperature of 50, 75 and 100 °C and equivalence ratio of 0.6–2.0 using a constant volume vessel. It is found that the laminar burning velocities of ethanol is the highest amongst the three fuels for the test conditions with respect to temperature and equivalence ratio, and it is approximately 30% faster compared with gasoline and DMF. This increase in flame speed is expected to lead to ethanol mixtures having shorter combustion durations, with the possibility of reduced NO_X emissions through reduced residence time and lower combustion temperature due to the charge cooling effect.

The study by Turner et al. [11] using a fuel blend of 85% ethanol and 15% gasoline, on the performance of a high compression ratio, super-charged spark ignition engine at wide open throttle conditions reported that the knock limit could be significantly raised due to the higher octane (RON) rating of ethanol (109) compared to gasoline (95). This allowed for the engine thermal efficiency to be increased (3–4% points) through the use of more favourable (closer to MBT) spark timings. The high latent heat of vaporisation was also effectively used by injecting a proportion of the fuel prior to the supercharger. This reduced the temperature rise across the supercharger and when 40% or more of the fuel was injected prior to the supercharger the temperature rise was reduced to zero, eliminating the need for an inter-cooler.

It is reported by Kar et al. [12] that the addition of ethanol to gasoline causes a non-linear change in the vapour pressure of the resulting mixtures. Although ethanol has a lower vapour pressure than that gasoline (see Table 2) as the ethanol content is increased up to 30% the vapour pressure increases, but further ethanol addition then causes a reduction in vapour pressure. This phenomenon causes the maximum cooling effect to be seen for approximately 50% ethanol content because of the competing factors of increasing enthalpy of vaporisation (low blends) and reducing vaporisation (lower vapour pressure for high blends). This suggests that the level of evaporation of impinged fuel from the combustion chamber surfaces and the in-cylinder temperatures prior to combustion are likely to be non-linear with respect to ethanol addition, with respect to increased injection duration in the GDI engine.

The non-linear behaviour of the vapour pressure with respect to ethanol blending ratio is attribute to the formation of positive azeotropes [12,13] with some of the hydrocarbon species found in gasoline, such as toluene, n-hexane and n-heptane [14]. This causes the vapour pressure of the mixture to be greater than that of the constituent parts, and therefore the mixture does not obey Raoult's law. This azeotrope formation causes an improvement to the midrange distillation as shown by Al-Farayedhi et al. [6] and da Silva et al. [13].

Table 1
Engine geometry.

Bore × stroke (mm)	90.0 × 88.9	
Swept. volume (cm^3)	565.6	
Compression ratio (geometric)	11.5:1	
Fuel delivery (fuel pressure)	Direct injection (150 bar)	
Valves	Intake	Exhaust
Lift (mm)	10.5	9.3
Opens (°$bTDC_{GE}$)	16	214
Closes (°$aTDC_{GE}$)	234	36

Table 2
Emission measurement method used with the Horiba MEXA-7100DEGR gas analyser.

Emission	Measurement method
HC	FID (hot)
CO	NDIR (dry)
CO_2	NDIR (dry)
NO_X	CLD (dry)

The aim of the study reported in this paper is to investigate the effects of blending bio-ethanol at different ratios with gasoline in a direct injection (DI) engine, using a range of spark timings. A direct injection engine is used in the study as injecting the fuel directly into the engine can help highlight the problems/benefits of the increased charge cooling offered by ethanol addition. Intake throttling is used to maintain the engine running at a constant speed of 1500 rpm at 3.4 bar IMEP. The effects investigated include combustion performance, regulated emissions and engine efficiency. The experimental system is described in the next section, followed by the presentation and discussion of the results, with a summary of the conclusions in the end of the paper.

2. Experimental apparatus and procedure

2.1. Engine and instrumentation

The test engine used for this study is a single-cylinder 4-stroke spark-ignition research engine. The cylinder head is a 4-valve single-cylinder Jaguar Spray-guided DI unit of similar design to their production naturally aspirated V8 engine [15], The DI system consists of a six hole injector, centrally mounted in the cylinder head and the fuel pressure is generated by a piston type accumulator that is charged with oxygen-free nitrogen. This system is used as it eliminates pressure fluctuations that are often associated with piston pumps. Both the intake and exhaust camshafts are fitted with an in-house developed, belt driven variable cam timing (VCT) system. A summary of the engine geometry is shown in Table 1 below. The engine was connected to a DC dynamometer with a speed sensing control system so a constant engine speed could be maintained for all of the tests in this study.

In-cylinder pressure measurements were made with a Kistler water cooled pressure transducer type 6041A fitted flush with the cylinder head wall, connected to a National Instruments data recording card via a Kistler 5011 charge amplifier. Samples were taken at 0.5CAD intervals for 300 consecutive cycles.

Lambda control was achieved by using an ETAS LA4 lambda meter connected to a heated Bosch oxygen sensor. The lambda meter was configured for each fuel blend by inputting the carbon/hydrogen, carbon/oxygen and stoichiometric air/fuel ratios for each individual fuel blend. The injection timing and pulse width was controlled by the operator via a LabVIEW script.

2.2. Emissions and fuel measurement

The gaseous emissions were measured with a Horiba MEXA-7100DEGR gas analyser incorporating a heated line and heated pre-filter. The analyser uses the methods shown in Table 2 for measuring the different exhaust gas components. The outputs from the analyser were connected to a National Instruments data recording card. Samples were recorded at a rate of 10 Hz for 30 s. It should be noted that although the authors are aware of the limitations of measuring oxygenated hydrocarbons with an FID, no correction to the HC measurements has been applied in this study. This is because for the correction factor to be accurate and correct the hydrocarbons emissions would have to by fully speciated and the relative concentrations of these species would need to be known.

The recorded data was processed in MATLAB using an in-house developed script to calculate engine load and stability, heat release analysis, indicated efficiency and specific emissions. The fuel consumption was calculated by relating the air inducted by the engine (measured with a positive displacement rotary flow meter) and the lambda value.

2.3. Test procedure

The engine was started and warmed-up using gasoline. Once the oil and water temperatures were in the range of 85 ± 3 °C and 93 ± 3 °C, respectively, the engine was then operated in DI mode using the ethanol blends. The intake air temperature was maintained at 33 ± 3 °C. All tests were conducted at an engine speed of 1500 rpm and a load of 3.4 bar IMEP (equivalent to 2.63 bar BMEP for a representative multi-cylinder production engine).

2.4. Definition of tests

Before the data reported in this paper was taken, initial tests were conducted using low ethanol blends (up to 30% ethanol in volume) to identify suitable injection strategies, involving both single and split injections respectively. The single injection strategies included standard early homogeneous and late (compression stroke) injections. Two different split injection strategies were investigated. For these the first injection occurred just after intake valve opening (IVO), with the second injection occurring either before or after intake valve closing (IVC). The two injection strategies chosen were the single homogeneous injection and the split injection where the second injection occurred after EVC, these are summarised in Table 3 along with the spark timings and fuel blends used for this study. Note that TDC is refers to the end of the compression stroke. The properties of the fuels used in the experiment are listed in Table 4.

Table 3
Test conditions.

Fuel blends (%$_{Vol.}$ ethanol)	0, 10, 20, 30, 50, 85, 100		
Spark timing (°bTDC)	19, 24, 29, 34[a], 39		
Injection strategies	No. of injections	SoI (°bTDC)	Designation
	Single	280	280
	Double[b]	1st 371 2nd 141	371/141
Stoichiometry	$\lambda = 1$		
Engine speed (rpm)	1500		
IMEP (bar)	3.4		

[a] MBT for standard gasoline, single injection.
[b] Equal injection duration.

Table 4
Fuel properties.

	Typical gasoline	Bio-ethanol
Octane no. (RON)	95	~110
LHV (MJ/kg)	43.0	26.8
$AFR_{Stoich.}$	14.48	8.96
Enthalpy of vaporisation (kJ/kg)	300	840.2
Density @ 15 °C	0.7387	0.7904
IBP (°C)	28.6	78
FBP (°C)	196.3	
Vapour pressure @ 20 °C (kPa)	~55	5.9 [12]
Laminar flame velocity @ 100 kPa, 325 K (cm/s)	~33 [7]	~39 [7]

3. Results and discussion

3.1. Combustion

The combustion initiation duration (CID) (defined as the time between spark discharge and 5% MFB) is shown in Fig. 1 below. It can be seen that for the 280SoI case SoC (defined as 5% MFB) tends to advance (reduced CID) as the ethanol content is increased. This is caused by ethanol having a faster laminar flame velocity [7] and hence the early laminar flame growth occurs at a faster rate, irrespective of the fact that the higher latent heat of ethanol means a lower in-cylinder temperature which has offset the speed of the flame growth.

For the 371/141SoI case it can be seen that for up to 30% ethanol content the effect on SoC is generally small. It can also be noted that for up to 30% ethanol content SoC is advanced (shorter CID) compared to the 280SoI case. This can be related to the time available for mixture heat recovery. With some of the fuel being injected very early in the cycle (before TDC_{GE}), there is more time available for heat recovery. Relating CID to heat recovery is reinforced by observation of the CID's relative to the spark timing. The earlier the spark timing is the shorter the time available for heat recovery. It can be seen that the CID for a spark timing of 39° bTDC is approximately 5° longer than that for a spark timing of 19° bTDC.

With split injection, increasing the ethanol content from 30% increases CID which peaks at 85% ethanol content. This could be caused by an increased amount of fuel impingement on the piston crown resulting from the very early (around TDC) first injection and the increased injection durations required for the higher ethanol blends (due to lower energy density) coupled with the reduction in the fuels volatility (vapour pressure). This reduced amount of vapour and increased wall impingement of fuel could result in a leaner mixture being present in the vicinity of the spark plug at the point of spark discharge. Pure ethanol has a slightly reduced CID compared to 85% ethanol content, which can be attributed to the removal of all heavy fuel fractions and thus leading to more complete evaporation from the piston crown. If leaner mixtures are present in the vicinity of the spark plug at the point of spark discharge, the CID is likely to be longer as the laminar flame speed of lean mixtures ($\varphi < 1$) of both ethanol and gasoline are slower than those for stoichiometric mixtures.

The early combustion duration, defined as 5–50% MFB duration, is shown below in Fig. 2. This duration is presented because the position of 50% MFB is often used to locate the combustion phasing. The 50% point is also a more reliable point to extract form the data as the 90% and 95% points lie in a generally flat area of the MFB curve and as such are more susceptible to noise and cycle tot cycle variations. As previously stated, ethanol has a faster laminar flame speed than that of gasoline, so it might be expected that as the ethanol content increases the combustion duration will reduce. The relevance of this increase in flame speed however has to be

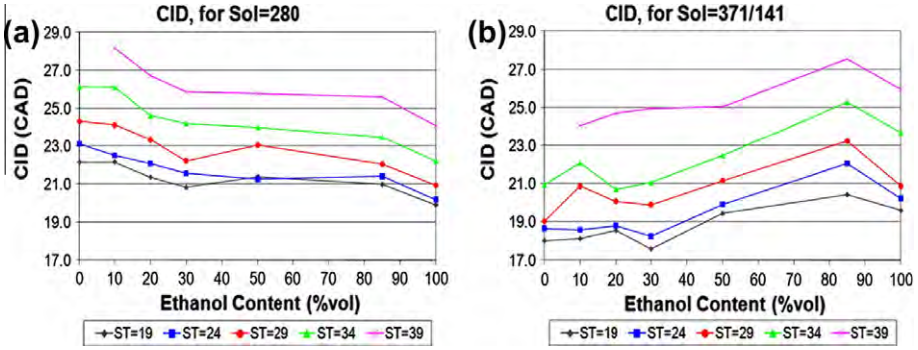

Fig. 1. CID with varied spark ignition timings: (a) single and (b) split injection strategies.

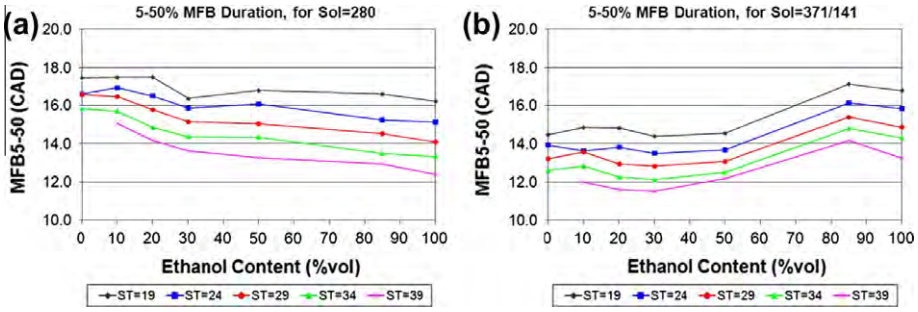

Fig. 2. 5–50% MFB duration with varied spark ignition timings: (a) single and (b) split injection strategies.

considered when applied to combustion in an engine, i.e., the turbulent speed of the bulk gas the flame is moving through has to be added to the laminar flame speed, with the influence of the gas temperature, in order to obtain the true engine flame speed. It can be seen that for both injection strategies as the combustion (5% MFB) is advanced (by either spark timing or fuel blend effects) the combustion duration is reduced. This is because more combustion is occurring in a smaller volume (piston at or close to TDC) and hence the temperature rise is greater. This increase in temperature further promotes combustion, reducing the duration.

Combustion stability is presented here as COV of IMEP and is shown in Fig. 3. It can be seen that combustion stability generally follows the same trend as that of combustion duration for both injection strategies. This can be correlated to in-cylinder flow and piston movement. The faster the combustion is, the less time there is for the flame front to be influenced by in-cylinder motion and gas expansion, and hence resulting in greater stability. At notable exception to this is for the most advanced spark timing (39° bTDC), were the combustion stability is lower than that expected from the combustion duration. An explanation for this could be that because of the reduced mixing time the mixture is not fully homogeneous (particularly for split injection) which results in variation form one cycle to the next.

Combustion efficiency (calculated from CO and HC in the exhaust stream) [16] is presented below in Fig. 4. It can be seen for the 280SoI case combustion efficiency generally improves with increased ethanol content, but there is little difference between 30% and 85% ethanol. This flattening of the combustion efficiency response is likely to be due to the offset caused by the reduction in exhaust temperature with increasing blend ratios as presented later, causing less CO oxidation in the expansion stroke. The combustion efficiencies for the 371/141SoI case up to 50% ethanol content are almost identical to those of the 280SoI case. The influence of mixing time has probably played a part, and it is reflected by the variation of combustion efficiency relative to spark timing – as the spark timing is advanced (mixing time reduced) the combustion efficiency reduces. For the 371/141SoI case there is a considerable reduction in combustion efficiency for 85% and 100% ethanol. This is thought to be caused by fuel impingement on the piston and mixture in-homogeneity when the injection became excessively

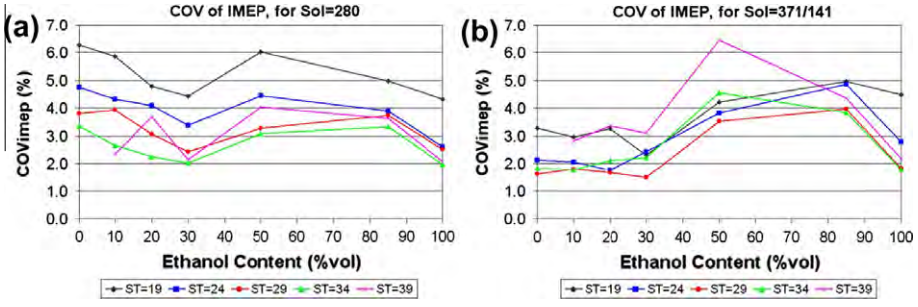

Fig. 3. COV_{IMEP} with varied spark ignition timings: (a) single and (b) split injection strategies.

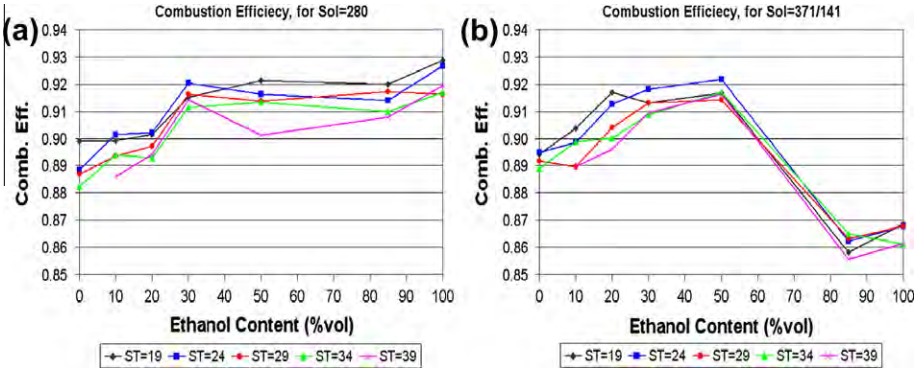

Fig. 4. Combustion efficiency with varied spark ignition timings: (a) single and (b) split injection strategies.

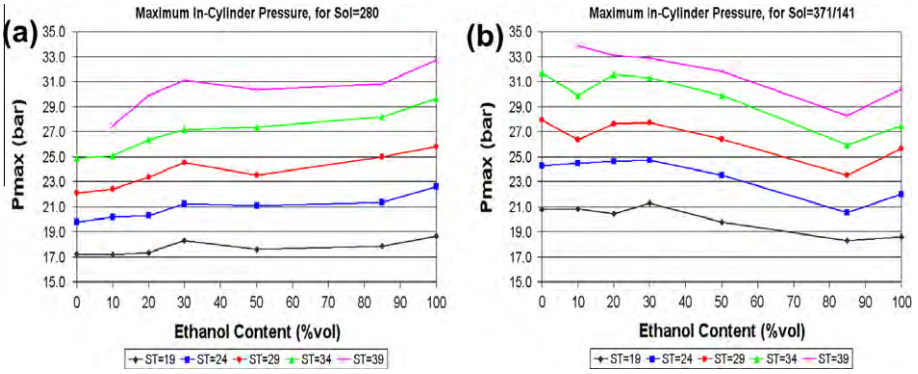

Fig. 5. Peak in-cylinder pressure with varied spark ignition timings: (a) single and (b) split injection strategies.

long for the high ethanol content and the phenomena will be discussed in more detail in the section on carbon monoxide emissions.

It is generally reported [1,3,17] that the in-cylinder temperatures reduce with the addition of ethanol, because ethanol has a lower adiabatic flame temperature and the higher heat of vaporisation increasing charge cooling. Peak in-cylinder temperature can be inferred from peak in-cylinder pressure but subject to some assumptions and uncertainties, and thus peak in-cylinder pressure is presented in Fig. 5 to assist the data interpretation.

It can be seen for the 280SoI case that the peak in-cylinder pressure (and therefore temperature) increases as the ethanol content increases to 30%, then levels out up to 85% ethanol and then increases again for pure ethanol. In general, the trends of the data in Fig. 5 are highly correlated to the combustion phasing (Fig. 1) and very similar to that of combustion efficiency (Fig. 4). For the 371/141SoI case up to 85% ethanol content the peak in-cylinder pressure (and therefore temperature) decreased before increasing slightly for pure ethanol.

Exhaust temperature is an important parameter as it concerns the late oxidation of HC and CO and the effectiveness of exhaust aftertreatment devices. It can be seen from Fig. 8 that for the 280SoI case, as the ethanol content is increased up to 85%, the exhaust temperature reduces and then increases slightly for pure ethanol. The advanced spark timings lead to lower exhaust temperatures as expected and this is mainly because with advanced combustion there is a longer gas expansion between the end of combustion and the exhaust valve opening. However the combustion phasing for 30–85% ethanol content is almost constant, whereas the exhaust temperature reduces as the fuel blend ratio increases. This can be attributed in general to the shorter burn duration of ethanol blends in addition to the lower adiabatic flame temperature. There is a very small increase in exhaust temperature for pure ethanol despite the advance in combustion phasing. The only explanation is that it is associated with the increase of peak combustion gas pressure (and thus temperature) as shown in Fig. 5.

For the 371/141SoI case the exhaust temperature, shown in Fig. 6, is generally unaffected by ethanol addition up to 30%. This is because up to 30% ethanol content the combustion phasing and in-cylinder temperatures remain constant. The exhaust temperature reduces for 50% ethanol content and then increases again as the ethanol content increases. The exhaust temperature for pure ethanol is similar to that of pure gasoline, as the results of the competing factors in maintaining the same load condition. It is also noted that the exhaust temperatures for up to 30% ethanol content are lower for the 371/141SoI case compared to the 280SoI case. Again the effect of spark timing on exhaust temperature is clear, with the more advanced spark timings leading to lower exhaust temperature through increased gas expansion and heat loss. The influence by the trend of combustion phasing is also evident, with the 371/141SoI case having more advanced combustion and thus lower exhaust temperature in general.

3.2. Emissions

The level of NO_X emissions is exponentially dependant on the in-cylinder temperature, as the in-cylinder temperature increases the rate of NO_X formation is increased. This trend is observed in Fig. 7a and b for both of the injection strategies, with the NO_X plot having the same shape as the peak in-cylinder pressure plot and hence temperature.

For both cases there is also a general reduction in NO_X emissions when the blending ratio is increased. However there is a small peak

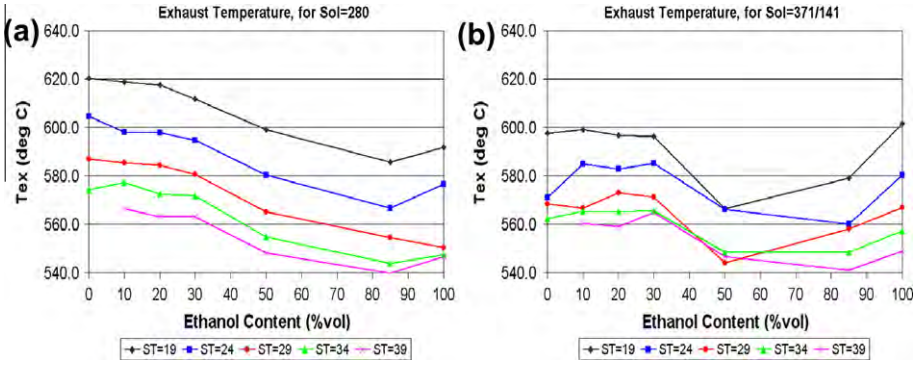

Fig. 6. Exhaust temperature with varied spark ignition timings: (a) single and (b) split injection strategies.

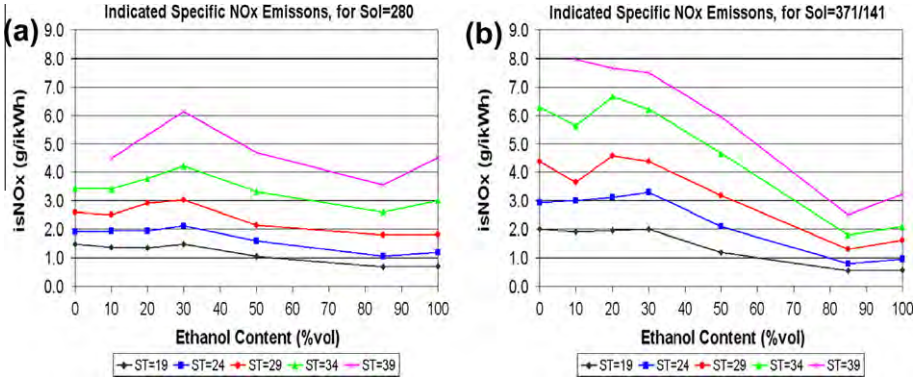

Fig. 7. NO_X emissions with varied spark ignition timings: (a) single and (b) split injection strategies.

at 30% ethanol content for the 280SoI case, which gets more pronounced as the spark timing is advanced, with the level then reducing as the ethanol content is increased. The peak at 30% ethanol content can be related to increase in peak in-cylinder temperature indicated by the peak in-cylinder pressure in Fig. 5 between pure gasoline and 30% ethanol content. For the 280SoI case the trend between 30% and 85% ethanol content could be because of the reduction in flame temperature as seen by the reduction in exhaust temperature. The NO_X level then increases slightly for pure ethanol and this is because of the combustion being advanced leading to a higher in-cylinder pressure and temperature compared to that of 85% ethanol. While for the 371/141SoI case, the trend follows the in-cylinder pressure very closely.

The hydrocarbon emissions are shown below in Fig. 8. It can be seen that both injection strategies lead to very similar (in both shape and value) trends for HC emissions versus both fuel blend and spark timing. There is an almost linear reduction in HC emissions with the increase in ethanol content. There are three factors influencing this result, i.e., mixing of the air/fuel mixture, the molecular weight of the fuel, and the sensitivity of an FID analyser towards oxygenated hydrocarbons.

The reduced sensitivity of an FID to oxygenated hydrocarbons is reported by Wallner and Miers [3] and Price et al. [18] cites the work by Cheng et al. [19], which gives FID responses (normalised to n-heptane) for various hydrocarbon families/species. It can be seen for alkanes all of the carbon atoms are detected. For aromatics and alkenes the response drops slightly to 97% and 95% respectively. Whereas for oxygenated compounds such as aldehydes and alcohols the FID response is reduced significantly, with ethanol giving a response of 83%.

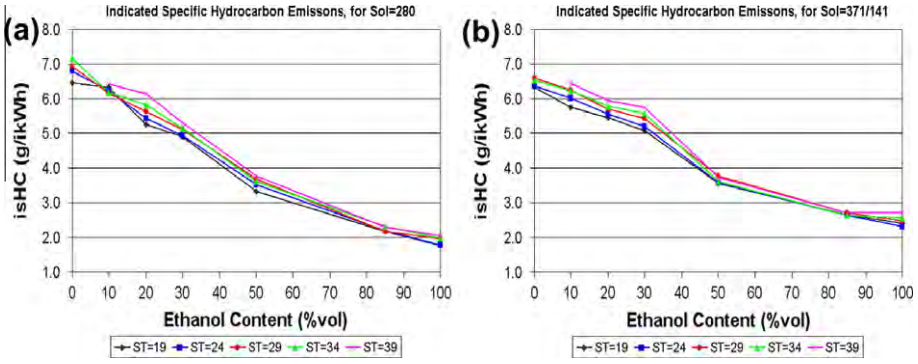

Fig. 8. Hydrocarbon emissions with varied spark ignition timings: (a) single and (b) split injection strategies.

It can be seen that as the spark timing is advanced the hydrocarbon emissions increase. This is caused by two mechanisms, the first being that the increased in-cylinder pressure (from advanced combustion) causes a greater mass of hydrocarbons to be trapped in the crevice volumes. The second mechanism is that the lower exhaust temperature (resulting from advanced combustion) causes less oxidation to take place as the trapped hydrocarbons get released (in the exhaust stroke) from the crevice volumes.

The similarity of emissions for both injection strategies and near linear response to ethanol addition suggests that the reduction in the fuels molecular weight (caused by the addition of ethanol) and the reduced ability of an FID to detect oxygenated hydrocarbons are the main causes for the trends in HC level seen.

The carbon monoxide emissions for the 280SoI case tend to reduce as the ethanol content is increased, as shown in Fig. 9, and generally the lowest CO emissions come from the retarded spark timings. However the latest (19° bTDC) spark timing does not follow this trend. A possible cause for this could be reduced in-cylinder temperatures seen with this perhaps over retarded spark timing being insufficient for the complete oxidation of CO to CO_2. Another factor that could explain the reduction in the CO emissions with ethanol addition is that the ethanol fuel molecule is oxygenated; hence more oxygen is available for complete combustion to occur. There is a slight flattening of the curve between 30% and 85% ethanol content for all spark timings, with the reduction of CO partially offset by the reduction in exhaust temperature resulting in less CO oxidation.

For the 371/141SoI case the CO emissions up to 30% ethanol content are very similar to those for the 280SoI case, with the reasons for this being the same as those given above. The significant increase of CO for 85% and pure ethanol can be attributed to the reduction in fuel volatility and the expected increase in fuel impingement on the piston crown caused by the very early first injection. The slight reduction for pure ethanol is thought to be caused by the removal of all high boiling point fractions that are present in gasoline. Another reason for the increase in CO for the higher ethanol blends could arise from reduced mixing thus reduced homogeneity associated with the longer injection duration. The combustion of rich regions and flame quenching in overly lean regions is expected to increase CO levels.

3.3. Efficiency

Indicated efficiency is being presented here instead of specific fuel consumption because of the varying degree of oxygenation of the fuels used and the impact this has on the resulting gravimetric heating value (~43 MJ/kg for gasoline and ~27 MJ/kg for ethanol).

Indicated efficiency is presented in Fig. 10 and it can be seen for the 280SoI case that as the ethanol content is increased the indicated efficiency also increases. This can be attributed to the increase in combustion efficiency (Fig. 4). In general, as the ethanol content is increased the spark timing has to be retarded (although these spark timings are not necessarily MBT timings) to achieve the highest efficiency. This is because as the ethanol content is increased the combustion initiation duration and the main combustion duration are both reduced, resulting in the need to delay the start of combustion.

For the 371/141SoI case indicated efficiency is generally unaffected by ethanol addition despite the increase in CO emissions for the higher ethanol blends. The increased CO levels would indicate a lower combustion efficiency (Fig. 4b). This would be accompanied by a reduction in the work done during the expansion stroke through an increase in the ratio of specific heats (γ) (CO replaces CO_2), though CO represents only a small percentage of the in-cylinder gasses and therefore the change in γ would be small. This shows that the indicated efficiency has clearly been dominated by a combination of factors, giving rise to the observed trend. One of these factors affecting indicated efficiency is pumping losses. If the combustion efficiency is reduced more fuel needs to

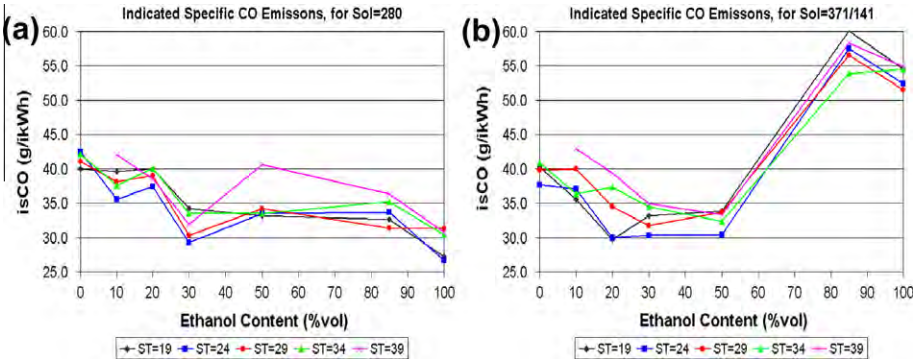

Fig. 9. Carbon monoxide emissions with varied spark ignition timings: (a) single and (b) split injection strategies.

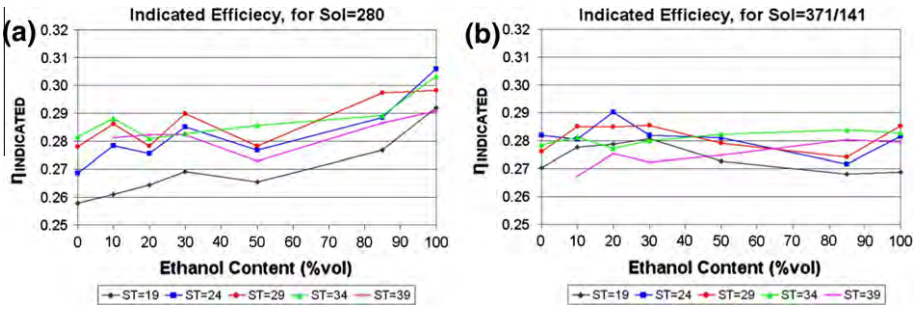

Fig. 10. Indicated efficiency with varied spark ignition timings: (a) single and (b) split injection strategies.

be delivered to maintain load, with the throttling valve being opened more to maintain stoichiometery. This reduction in throttling results in reduced pumping losses, which goes someway to countering the reduction in combustion efficiency.

4. Conclusions

An experimental investigation has been conducted using different blending-ratios of bio-ethanol/gasoline with respect to spark timing and injection strategies, on a direct injection spark ignition engine at a part load and speed condition. The main characteristics of combustion and emissions of the engine revealed by this study when the ethanol/gasoline blend ratio increased from 0% to 100% compared with the gasoline baseline in general are as follows.

1. Reduced combustion initiation duration because of higher laminar flame velocities.
2. Faster combustion and thus higher in-cylinder pressure because of a combination of advanced combustion and higher flame speeds.
3. Improved combustion stability resulting from advanced and faster combustion being less susceptible to in-cylinder motion.
4. Improved combustion efficiency as a result of better evaporation (reduction of heavy fractions) and mixing coupled with the presence of oxygen within the fuel molecule.
5. Similar or reduced levels of NO_X emissions.
6. Reduced CO emissions resulting from improved combustion efficiency (single injection).
7. Increased engine efficiency.
8. Split injection strategies, however, can considerably modify the combustion and emission characteristics. They can provide reduced combustion initiation duration and improved combustion stability for lower ethanol blends ($\leqslant 30\%_{Vol.}$) but the situation deteriorates for higher ethanol blends for certain chosen injection timings, with the postulated cause being fuel impingement on the piston caused by the early injection.

Acknowledgments

The authors acknowledge the financial supports from Shell Global Solutions and the Engineering and Physical Sciences Research Council (EPSRC) under the grant EP/F061692/1. The authors wish to thank their colleagues in the Future Engine and Fuels Lab and specially Jaguar Land Rover for technical support on the engine test facilities.

References

[1] Nakata K, Utsumi S, Ota A, Kawatake K, Kawai Y, Tsunooka T. The effect of ethanol fuel on a spark ignition engine. SAE paper 2006-01-3080; 2006.
[2] Wyszynski LP, Stone R, Kalghatgi GT. The volumetric efficiency of direct and port injection gasoline engines with different fuels. SAE paper 2002-01-0839; 2002.
[3] Wallner T, Miers SA. Combustion behavior of gasoline and gasoline/ethanol blends in a modern direct-injection 4-cylinder engine. SAE paper 2008-01-0077; 2008.
[4] Brinkman N, Halsall R, Jorgensen SW, Kirwan JE. The development of improved fuel specifications for methanol (M85) and ethanol (E85). SAE paper 940764; 1994.
[5] Gardiner DP, Rao VK, Bardon MF, Dale JD, Smy PR, Haley RF, Dawe JR, Battista V, Sub-zero cold starting of a port-injected M100 engine using plasma jet ignition and prompt EGR. SAE paper 930331; 1993.
[6] Al-Farayedhi AA, Al-Dawood AM, Gandhidasan P. Effects of blending crude ethanol with unleaded gasoline on exhaust emissions of SI engine. SAE paper 2000-01-2857; 2000.
[7] Hara T, Tanoue K. Laminar flame speed of ethanol, n-heptane, iso-octane air mixtures. SAE paper no. 2006-05-0409; 2006.
[8] Beeckmann J, Röhl O, Peters N. Numerical and experimental investigation of laminar burning velocities of iso-octane, ethanol and n-butanol. SAE paper 2009-01-2784; 2009.
[9] Farrell JT, Johnston RJ, Androulakis IP. Molecular structure effects on laminar burning velocities at elevated temperature and pressure. SAE paper 2004-01-2936; 2004.
[10] Tian G, Daniel R, Li H, Xu HM, Shuai S, Richards P. Laminar burning velocities of 2,5-Dimethylfuran compared with ethanol and gasoline. Energy Fuels 2010;24:3898–905. doi:10.1021/ef100452c1.
[11] Turner JWG, Pearson RJ, Holland B, Peck R. Alcohol-based fuels in high performance engines. SAE paper 2007-01-0056; 2007.
[12] Kar K, Last T, Haywood C, Raine R. Measurements of vapor pressures and enthalpies of vaporization of gasoline and ethanol blends and their effects on mixture preparation in an SI engine. SAE paper 2008-01-0317; 2008.
[13] da Silva R, Cataluña R, de Menezes EW, Samios D, Piatnicki CMS. Effect of additives on the antiknock properties and Reid vapor pressure of gasoline. Fuel 2005;84:951–9.
[14] Lang NA. Lange's handbook of chemistry. McGraw-Hil; 1967.
[15] Sandford M, Page G, Crawford P. The all new AJV8. SAE paper 2009-01-1090; 2009.
[16] Heywood JB. Internal combustion engine fundamentals. McGraw-Hill; 1988.
[17] Serras-Pereira J, Aleiferis PG, Richardson D, Wallace S. Characteristics of ethanol, butanol, iso-octane and gasoline sprays and combustion from a multihole injector in a DISI engine. SAE paper 2008-01-1591; 2008.
[18] Price P, Twiney B, Stone R, Kar K, Walmsley H. Particulate and hydrocarbon emissions from a spray guided direct injection spark ignition engine with oxygenate fuel blends. SAE paper 2007-01-0472; 2007.
[19] Cheng WK, Summers T, Collings N. The fast-response flame ionization detector. Prog Energy Combust Sci 1998;24:89–124.